

Nitrogen isotopes in AGB carbon stars and presolar SiC grains: a challenge for stellar nucleosynthesis

R. P. Hedrosa¹, C. Abia¹

Departamento de Física Teórica y del Cosmos, Universidad de Granada, 18071 Granada,
Spain

M. Busso^{2,3}

Dipartimento di Fisica, Università di Perugia, 06123 Perugia, Italy
INFN, Sezione di Perugia, 06123 Perugia, Italy

S. Cristallo⁴

INAF, Osservatorio di Collurania, 64100 Teramo, Italy

I. Domínguez¹, S. Palmerini¹

Departamento de Física Teórica y del Cosmos, Universidad de Granada, 18071 Granada,
Spain

B. Plez⁵

Laboratoire Univers et Particules de Montpellier, Université Montpellier II, CNRS, 34095
Montpellier, France

and

O. Straniero⁴

INAF, Osservatorio di Collurania, 64100 Teramo, Italy

Received _____; accepted _____

ABSTRACT

Isotopic ratios of C, N, Si, and trace heavy elements in presolar SiC grains from meteorites provide crucial constraints to nucleosynthesis. A long-debated issue is the origin of the so-called A+B grains, as for them no stellar progenitor has so far been clearly identified on observational grounds. We report the first spectroscopic measurements of $^{14}\text{N}/^{15}\text{N}$ ratios in Galactic carbon stars of different spectral types and show that J- and some SC-type stars might produce A+B grains, even for ^{15}N enrichments previously attributed to novae. We also show that most mainstream (MS) grains are compatible with the composition of N-type stars, but might also descend, in some cases, from SC stars. From the theoretical point of view, no astrophysical scenario can explain the C and N isotopic ratios of SC, J and N-type carbon stars together, as well as those of many grains produced by them. This poses urgent questions to stellar physics.

Subject headings: stars: carbon — stars: abundances — nuclear reactions, nucleosynthesis, abundances

1. Introduction

After the exhaustion of He in the core, stars of mass $0.8 \lesssim M/M_{\odot} \lesssim 8$ become very luminous and cool and climb the so called Asymptotic Giant Branch (AGB). AGB stars are powered by two nuclear shells, burning H and He alternatively; He, in particular, burns recurrently in short explosive events called thermal pulses. After most of them, the convective envelope penetrates downward bringing to the surface H- and He-burning products in a phenomenon called third dredge up (TDU). Carbon is the main product of He burning, thus AGB stars, from their initially O-rich composition, get enriched in carbon (and in other He-burning products, like s-elements). For suitable values of the envelope mass (eroded by mass loss) AGB stars finally achieve an abundance ratio $C/O > 1$ (by number), in which case they become carbon stars of a class called C(N) (or N-type). This typically occurs between 1.5 and 3-4 M_{\odot} for solar chemical composition (Abia et al. 2002; Cristallo et al. 2011). Above $M \gtrsim 4 M_{\odot}$ stars cannot become carbon rich, both because of the large envelope mass to pollute, and because the hot temperature at its base induces CN-cycling, burning the dredged-up carbon in a process called hot bottom burning, or HBB (Renzini & Voli 1981).

It was inferred spectroscopically that composition changes induce a spectral type evolution along the sequence (Wallerstein & Knapp 1998): $M \rightarrow MS \rightarrow S \rightarrow SC \rightarrow C(N)$ although there are some doubts on the nature of SC stars, see below. The composition determines the type of condensates forming in the circumstellar envelope. Oxides and silicates form in O-rich AGB stars (M, MS, S) while C-rich stars are parents to SiC and graphite dust. After its ejection into the interstellar medium by stellar winds, this cosmic dust can be trapped in meteorites, that are now recovered in the Solar System. Among these dust particles, SiC grains are probably the best studied ones (see e.g. Davis 2011). They are classified on the basis of their nitrogen, carbon and silicon isotopic ratios (see

e.g., Nittler 2003). The so-called mainstream (MS) grains which constitute 93% of all SiC grains, show a huge range in the $^{14}\text{N}/^{15}\text{N}$ ratio (from 10 to 10000). Moreover, these grains show isotopic anomalies that can be only explained if they have been formed from material exposed to s-process nucleosynthesis, which is thought to occur during the AGB phase of low-mass stars (see e.g., Straniero, Gallino & Cristallo 2006). On the other hand, grains of type A+B ($\sim 4\%$ of presolar SiC) show also a large spread in the N ratio, but low $^{12}\text{C}/^{13}\text{C}$ ratios (< 10); their origin is still unclear (Amari et al. 2001).

Spectroscopically, C(N) stars show strong CN and C_2 bands. They also display absorption lines of F and s-elements, whose enrichment is in good agreement with stellar and nucleosynthesis models (Abia et al. 2002, 2010; Cristallo et al. 2011), so that the AGB evolutionary stages are thought to be well understood. Their $^{12}\text{C}/^{13}\text{C}$ ratios are typically $\gtrsim 30$, averaging at ~ 60 . Other types of carbon-rich giants exist, but of a more unclear origin. Among them, SC-type stars show molecular bands indicating C/O ratios close to unity; s-element enhancements are not always present and the $^{12}\text{C}/^{13}\text{C}$ ratios range from CN-cycle equilibrium (3–4) up to ~ 100 . A few SC stars are super Li-rich (Abia & Isern 1997), with Li abundances larger by 4-5 orders of magnitude than for C(N) giants. They also show the largest F enhancements¹, $[\text{F}/\text{Fe}] \sim 1$ (Abia et al. 2010), in solar metallicity ($[\text{Fe}/\text{H}] \sim 0$) carbon stars. Furthermore, they seem to be on average more luminous than C(N) giants (Guandalini 2008), suggesting stellar masses $\gtrsim 4 M_{\odot}$, thus casting doubts on their position in the spectral sequence going from M to C(N) types. Another subgroup of carbon stars, the J-type, shows strong features of ^{13}C -bearing molecules, indicating $^{12}\text{C}/^{13}\text{C} \lesssim 15$. They have no s-element enhancement and are, in most cases ($\sim 80\%$), moderately Li-rich (Abia & Isern 1997). Their relation to the quoted spectral sequence

¹Here we adopt the definition $[\text{A}/\text{B}] = \log(N_{\text{A}}/N_{\text{B}}) - \log(N_{\text{A}}/N_{\text{B}})_{\odot}$ where $\log(N_{\text{A}}/N_{\text{H}})$ is the abundance by number of the element A.

is unclear. Several J stars ($\sim 30\%$) show infrared emission lines, associated with silicate dust: a peculiar property, given their C-rich composition, although chemical kinetics allows for the formation of O-based compounds in C-rich environments (Cherchenff 2011). The emission seems in any case to come from O-rich discs in binary systems (Chen et al. 2007), indicating binarity as a common property of these stars.

Here we derive for the first time the $^{14}\text{N}/^{15}\text{N}$ ratios in a sample of near solar metallicity Galactic carbon stars of different spectral types. Our analysis reveals that the N isotopic ratios in N-type stars cover nicely the range found in the mainstream SiC grains, while those derived in J- and SC-type support an origin for A+B grains in these peculiar stars. We discuss briefly the results in the framework of the standard AGB phase stellar evolution and conclude that no known evolutionary scenario can explain the full range of $^{14}\text{N}/^{15}\text{N}$ ratios found in these stars.

2. Observations and analysis

We obtained very high-resolution echelle spectra ($R \approx 170000$) of nineteen N-, eight J- and eight SC-type Galactic carbon stars of near solar metallicity with the SARG spectrograph at the 3.5m TNG telescope. The signal-to-noise ratio in the spectral region of interest ($\sim 8000 \text{ \AA}$) was typically $\gtrsim 300$. In this wavelength interval there are various $^{12}\text{C}^{15}\text{N}$ absorption features sensitive to the ^{15}N abundance. The CN line list by Hill et al. (2002) was improved to allow the identification of $^{12}\text{C}^{14}\text{N}$, $^{13}\text{C}^{14}\text{N}$, and $^{12}\text{C}^{15}\text{N}$ lines. First, wavelengths were improved using the energy levels of Ram, Wallace, and Bernath (2010) for $^{12}\text{C}^{14}\text{N}$, and of Ram et al. (2010) for $^{13}\text{C}^{14}\text{N}$. They were supplemented by wavelengths from Kotlar, Field, & Steinfeld (1980) or calculated by extrapolation of the molecular constants when needed. Isotopic shifts were computed for all isotopic combinations, using the usual isotope relationship for the Dunham coefficients (Townes & Schawlow 1995). It appeared

that $^{13}\text{C}^{14}\text{N}$ line positions computed in this way were systematically displaced relative to the laboratory data by Ram et al. (2010). We therefore anticipated that the line positions for other isotopologues would be shifted as well. We realized that the ratio of the computed isotopic shifts for 2 different isotopologues were close to a constant, i.e. $C_{25/34} \approx 0.73^2$ in the case of $^{12}\text{C}^{15}\text{N}$ and $^{13}\text{C}^{14}\text{N}$ in the spectral region of interest. We therefore computed a correction to our calculated $^{12}\text{C}^{15}\text{N}$ isotopic shift, scaling the difference for $^{13}\text{C}^{14}\text{N}$ between Ram et al.’s measurement and our calculated value of the isotopic shift with the $C_{25/34}$ factor. We could compare this calculation to observed $^{12}\text{C}^{15}\text{N}$ line positions kindly sent to us by R. Colin. The comparison showed a good agreement, sufficient to give us confidence in our identifications of isotopic lines in stellar spectra. The used features were carefully selected to avoid blending and excluding lines for which, the pseudo-continuum position was uncertain. Moreover, only $^{12}\text{C}^{15}\text{N}$ features in the linear part of the curve-of-growth were used. This resulted in a few useful lines located near 7980, 7985, 8030, 8038, and 8064 Å (see Table 1). For other molecular and atomic lines contributing in this region we used line lists from previous works (Abia et al. 2002, 2010). Stellar parameters (T_{eff} , gravity, metallicities, C/O and $^{12}\text{C}/^{13}\text{C}$ ratio) were taken from the literature (see references in Table 2). For some stars (see Table 2), carbon and oxygen abundances were derived from a few weak, unblended C_2 and CO lines in the 2.2 μm region using high signal-to-noise and resolution ($R \sim 65000$) spectra (kindly provided by K. Hinkle) obtained at the 4 m Kit Peak Observatory telescope using a Fourier transform spectrograph. Then, the N abundance as well as the final C/O ratio were derived from CN lines in the 8000 Å region in an iterative way until agreement with the values obtained in the infrared spectral range

²Isotopic shifts are calculated relative to the majority species $^{12}\text{C}^{14}\text{N}$. $C_{25/34} = (\lambda_{25} - \lambda_{24})/(\lambda_{34} - \lambda_{24})$ is the mean ratio of the isotopic shifts of lines of the $^{12}\text{C}^{15}\text{N}$ and $^{13}\text{C}^{14}\text{N}$ isotopologues, for a given band.

was reached. We note however, that uncertainties in the absolute abundance of N within ± 0.3 dex does not affect the nitrogen ratio derived.

A C-rich spherical MARCS (Gustafsson et al. 2008) model atmosphere was chosen for each star according to its stellar parameters, and synthetic LTE spectra were calculated in the 8000 Å region, using the Turbospectrum v10.1 code (Plez 2012). Theoretical spectra were convolved with a Gaussian function with the corresponding FWHM to mimic the spectral resolution in each range plus the macroturbulence parameter (9-13 km s⁻¹). We used χ^2 **minimization techniques** to determine the ¹⁴N/¹⁵N ratios providing the best fit to each ¹²C¹⁵N feature. The goal was to fit not only the selected lines, but also the overall shape of the spectra. The N isotopic ratios thus derived were then combined to obtain an average. The N ratios obtained from the ¹²C¹⁵N features at $\lambda 7980$, and $\lambda 8064$ Å were considered twice in deriving this average. These features are the most sensitive to ¹⁴N/¹⁵N variations. In this way we measured reliable N isotopic ratios for 22 stars of our sample; in a few cases we did not detect ¹⁵N and for the rest we established lower limits on ¹⁴N/¹⁵N (see Table 2). In most cases, the overall uncertainty in the N ratios is estimated to be less than a **factor of four**. This mainly reflects the sensitivity to changes in the atmospheric parameters adopted, plus the dispersion in the ¹⁴N/¹⁵N ratio derived among the different features. This also includes the uncertainty in the placement of the spectral continuum ($\leq 3\%$) and in the calculated wavelength of the ¹²C¹⁵N features (≤ 15 mÅ). Thus, to minimize the errors we performed a relative line-by-line analysis with respect to the C(N) star LQ Cyg ($[^{14}\text{N}/^{15}\text{N}]_{LQ\text{Cyg}}$) for which we measured ¹⁴N/¹⁵N= 1170. For this star we obtained a very good global fit to its spectrum. The relative analysis reduced the dispersion in $[^{14}\text{N}/^{15}\text{N}]_{LQ\text{Cyg}}$ derived for a given star (see Table 2). We estimate a total uncertainty of ± 0.4 dex for $[^{14}\text{N}/^{15}\text{N}]_{LQ\text{Cyg}}$.

Figure 1 shows examples of synthetic fits to ¹²C¹⁵N features in four of the studied stars

with different $^{14}\text{N}/^{15}\text{N}$ ratios. Figure 2 shows the $^{14}\text{N}/^{15}\text{N}$ ratios derived for our sample stars (normalized to LQ Cyg) versus their $^{12}\text{C}/^{13}\text{C}$ ratios. Over-plotted (gray symbols) are the isotopic ratios measured in MS and A+B SiC grains (Hoppe et al. 1994; Amari et al. 2001; Hynes & Gyngard 2009). The black point indicates model N and C isotopic ratios for a $2 M_{\odot}$ AGB star of solar metallicity **at the time that it becomes** C-rich ($[^{14}\text{N}/^{15}\text{N}]_{LQ\text{Cyg}} \approx +0.2$, $^{12}\text{C}/^{13}\text{C} \approx 70$). These values derive from the combined action of the first dredge-up (RGB phase), where the $^{14}\text{N}/^{15}\text{N}$ ratio grows from the initial (solar) value, 470 (Marty et al. 2011) to ~ 1000 , and the subsequent evolution before the C-rich AGB phase. This includes some (small) contribution from non-convective (extra) mixing during the RGB phase, as required by observations (Palmerini et al. 2011). This point, plotted for $\text{C}/\text{O} = 1$, represents a *lower limit* of N isotopic ratios for solar metallicity C(N) stars. This limit slightly increases for increasing stellar mass and decreasing metallicity. Further extra-mixing during the AGB phase would move the point along the diagonal arrow, while more TDU episodes would increase the $^{12}\text{C}/^{13}\text{C}$ ratio along the right-hand arrow (see Fig. 2).

3. Results and discussion

Among the carbon stars studied, J-type giants are defined mainly by their low $^{12}\text{C}/^{13}\text{C}$ and by the absence of s-elements. Their spectra are difficult to analyze, showing broad lines and unidentified features that cannot be well reproduced. In spite of this, their C and N isotope ratios closely match those of the A+B grains (see Fig. 2). The observational uncertainties are large, but not enough to hamper this conclusion. This is therefore the first experimental, unambiguous evidence ascribing at least part of A+B grains to J stars, confirming previous qualitative hints (Amari et al. 2001). Interestingly enough, the fraction of A+B grains within all SiC grains ($\sim 5\%$) (Davis 2011) is very similar to that

of J-type stars among all Galactic AGB carbon stars ($\sim 4 - 10\%$) (Boffin et al. 1993; Barnbaum et al. 1996). We also identified, for the first time, a few (although two are lower limits) ^{15}N -rich ($^{14}\text{N}/^{15}\text{N} \lesssim 1000$, or $[^{14}\text{N}/^{15}\text{N}]_{LQCyg} \lesssim -0.07$) J stars (Fig. 2): an amazing result, with no explanation in red giant models, which invariably **predict** ^{14}N -rich envelopes. Notice that also the very low $^{12}\text{C}/^{13}\text{C}$ ratios ($\lesssim 4$), shared by many A+B grains and by some J stars, cannot be achieved by nucleosynthesis scenarios for red giants except in the case of HBB or extreme extra-mixing processes (see below). These however imply large ^{14}N production and O-rich environments. Low C and N isotopic ratios were so far obtained only in simulations of nova explosions (José et al. 2004); but apart from the fact that novae do not account for the entire range of C and N ratios of A+B grains³, there is no known connection between novae and J stars. Actually, until now very few carbon-rich grains can be really ascribed to novae (Gehrz et al. 1998).

On the other hand, we notice that almost all the data for C(N) stars lay above $^{14}\text{N}/^{15}\text{N} \gtrsim 1000$ (or $[^{14}\text{N}/^{15}\text{N}]_{LQCyg} \gtrsim -0.07$, Fig. 2) occupying the same region as many MS grains. As our detection limit is $[^{14}\text{N}/^{15}\text{N}]_{LQCyg} \lesssim +0.7$ (or $^{14}\text{N}/^{15}\text{N} \lesssim 5000$), we cannot even exclude the existence of C(N) stars with higher ^{14}N -enrichments, as shown by several MS grains. Since MS grains also show s-process signatures (Zinner et al. 1987; Gallino et al. 1990), they are believed to form in N-type stars. Data of C(N) stars confirm the large spread of N and C isotopic ratios measured in SiC grains, stressing our incapability to explain isotopic abundances for several grains and a few C(N) giants with any theoretical scenario proposed to date. For instance, the occurrence of any non-convective (extra) mixing episode, linking the envelope to regions where proton captures occur, would further increase $^{14}\text{N}/^{15}\text{N}$ up to values around 10^4 , and also lower the $^{12}\text{C}/^{13}\text{C}$ ratio (Nollet et al.

³Note nevertheless that Nittler & Hoppe (2005) reported a SiC grain with supernova isotope signatures but also low C and N ratios.

2003) (diagonal arrow in Fig. 2). Any such process would imply an anti-correlation between N and C isotopic ratios, but there is no evidence of this in N-type stars or in MS grains. Furthermore, the existence of grains with N isotopic ratios similar and/or lower than solar is not explained by stellar nucleosynthesis or galactic chemical evolution. This has been ascribed to isotopic fractionation or terrestrial contamination (Jadhav et al. 2012; Adande & Ziurys 2012) but now we have shown that some C(N) stars also lay on that region (although, being lower limits, their uncertainty prevents us from conclusive statements). The above situation, in any case, challenges our current understanding of stellar evolution.

Finally, SC-type carbon stars are rare ($\lesssim 1\%$ of AGB carbon stars), indicating very short evolutionary times or uncommon evolutionary paths. With a C/O ratio very close to unity, O-rich and C-rich grain formation still relies on poorly-known chemical kinetic processes (Cherchenff 2011). In fact, SC stars show little evidence of dust; and the solids that form include relatively uncommon species, like troilite (FeS) (Hony et al. 2002). They may represent a short transition from $C/O \lesssim 1$ to $C/O \gtrsim 1$ compositions; but then N and C isotopic ratios should be close to those of N-type stars and s-elements should always be enhanced. Instead, these stars are all ^{15}N -rich (with $^{14}\text{N}/^{15}\text{N} \lesssim 1000$), independently of their C isotope ratio; and s-element enhancements exist in some, but not all of them. While the composition of these stars is consistent with both the MS and A+B ^{15}N -rich grain groups, their origin is a mystery. It was suggested that they are massive ($\gtrsim 4 M_{\odot}$) O-rich AGB stars, forming C-rich envelopes only for a short time due to an efficient dredge-up (Frost et al. 1998). The suspected larger masses would explain the extreme Li enhancements observed in some of them through HBB and the Cameron & Fowler (1981) mechanism. However, if HBB were sufficiently active to produce a lot of Li, very low F, C/O and $^{12}\text{C}/^{13}\text{C}$ ratios and very large ($\gtrsim 10^4$) $^{14}\text{N}/^{15}\text{N}$ ratios would result, all clearly at odds with observations (Fig. 2). In general, therefore, the chemical pattern

of SC stars, including N isotopes, although in line with that of various presolar grains, cannot be explained by standard stellar evolution. Note that nuclear rate uncertainties in CNO cycling are **not large enough** to account for the peculiar isotopic abundances we measured. Perhaps some of these stars formed with initial $^{14}\text{N}/^{15}\text{N}$ ratios dispersed over a huge range, but physical paths leading to such a scenario are not known. Moreover, determinations of $^{14}\text{N}/^{15}\text{N}$ in the local interstellar medium (ISM) yield values for this ratio (290 ± 40) close to the terrestrial and solar ones, with a small gradient in distance moving away from the Galactic center ($21.1\pm 5.2 \text{ kpc}^{-1} + 123.8 \pm 37.1$) (Adande & Ziurys 2012). Although such measurements in the ISM are difficult, there seems to be no space for a wide dispersion of values. So far, tentative explanations of the huge range of N ratios in SiC grains assumed contamination either from terrestrial N or from cosmic-ray spallation (that should correlate with grain size and meteoritic age, respectively: Jadhav et al. (2012)). Alternatively, non-equilibrium chemistry in the ISM might trigger isotopic fractionation (Adande & Ziurys 2012; Bonal et al. 2012). However, all these suggestions are now in conflict with the evidence that anomalous nitrogen isotopic admixtures already existed in the parent C-rich red giants.

Summing up, our new data establish observationally, for the first time that, while C(N) stars are parents of MS grains with high $^{14}\text{N}/^{15}\text{N}$ ratios, J-type carbon stars might generate A+B grains and SC stars might be a source for the grains with low $^{14}\text{N}/^{15}\text{N}$ ratios. However, no known evolutionary scenario can explain all the whole resulting evidence. One might guess that some mixing/nucleosynthesis mechanism occurs during a stellar merging, producing peculiar stars as a result (Zhan & Jeffery 2013). However, this is a qualitative speculation and the underlying physics is still largely unexplored.

Results are mainly based on observations made with the Italian Telescopio Nazionale Galileo (TNG) operated on the island of La Palma by the Fundación Galileo Galilei of

INAF (Istituto Nazionale di Astrofisica) at the Spanish Observatorio del Roque de los Muchachos of the Instituto de Astrofísica de Canarias. We thank K. Eriksson and R. Colin for providing the C-rich atmosphere models and laboratory $^{12}\text{C}^{15}\text{N}$ line positions, respectively. This work has been partially supported by Spanish grants AYA2008-04211-C02-02 and AYA-2011-22460. S.C. and O.S. acknowledge funding from FIRB-MIUR 2008 (RBF08549F-002) and from PRIN-INAF 2011 Multiple populations in Globular Clusters: their role in the Galaxy assembly.

Facilities: TNG (INAF-IAC).

REFERENCES

- Abia, C. et al., 2010, *ApJ*, **715**, L94.
- Abia, C. et al., 2002, *ApJ*, **579**, 817
- Abia, C., & Isern, J., 2000, *ApJ*, **536**, 438
- Abia, C. & Isern, J., 1997, *MNRAS*, **289**, L11
- Adande, G.R. & Ziurys, L.M., 2012, *ApJ*, **744**, 194
- Amari, S., Nittler, L.R., Zinner, E., Lodders, K. & Lewis, R.S., 2001, *ApJ*, **559**, 463
- Barnbaum, C., Stone, R.P.S., 1996, *ApJS*, **105**, 419
- Boffin, H.M.J., Abia, C., Rebolo, R. & Isern, J., 1993, *A&AS*, **102**, 361
- Bonal, P., Hily-Blant, A.F. & Quirico, E., 2012, *Meteoritics and Planetary Science*
Supplement, **5226**
- Cameron, A.G.W. & Fowler, W.A., 1971, *ApJ*, **164**, 111
- Chen, P., Yang, X. & Zhang, P., 2007, *AJ*, **134**, 214
- Cherchneff, I., 2011, *A&A*, **526**, L11
- Cristallo, S. et al., 2011, *ApJ*, **197**, 17
- Davis, A.M., 2011, *Proc. Nat. Acad. Sci. USA*, **108**, 19143
- Frost, C.A., Cannon, R.C., Lattanzio, J.C., Wood, P.R. & Forestini, M., 1998, *A&A*, **332**,
L17
- Gallino, R., Busso, M., Picchio, G. & Raiteri, C. 1990, *Nature*, **348**, 298

- Gehrz, R.D., Truran, J.W., Williams, R.E. & Starfield, S., 1998, *PASP*, **110**, 3
- Guandalini, R. 2008, in *AIP Conference Proceedings*, **1001**, 339
- Gustafsson, B. et al., 2008, *A&A*, **486**, 951
- Hill, V., et al. 2002, *A&A*, **387**, 560
- Hony, S., Bouwman, J., Keller, L.P. & Waters, L.B.F.M., 2002, *A&A*, **393**, L103
- Hynes, K. M. & Gyngard, F., 2009, *Lunar Planet. Sci. Conf.*, **40**, 1198
- Hoppe, P., Amari, S., Zinner, E., Ireland, T. & Lewis, R. S., 1994, *ApJ*, **430**, 870
- Jadhav, M., Nagashima, K., Huss, G.R. & Ogliore, R.C., 2012, in *43rd Lunar Planet Sci. Conf.*, **2826**
- José, J., Hernanz, M., Amari, S., Lodders, K. & Zinner, E., 2004, *ApJ*, **612**, 414
- Kotlar, A.J., Field, R.W., & Steinfield, J.I., 1980, *Journal of Molecular Spectroscopy*, **80**, 86
- Lambert, D.L., Gustafsson, B., Eriksson, K. & Hinkle, K. H., 1986, *ApJS*, **62**, 737
- Marty, B., Chaussidon, M., Wiens, R.C., Jurewicz, A.J.G. & Burnett, D.S., 2011, *Science*, **332**, 1533
- Nittler, L. R., 2003, *E & PSL*, **209**, 259
- Nittler, L. R., & Hoppe, P., 2005, *ApJ*, **631**, L89
- Nollet, K. M., Busso, M. & Wasserburg, G.J., 2003, *ApJ*, **582**, 1036
- Ohnaka, K., & Tsuji, K., 1996, *A&A*, **310**, 933
- Palmerini, S., La Cognata, M., Cristallo, S., & Busso, M., 2011, *ApJ*, **729**, 3

- Plez, B., 2012, *Astroph. Source Code Library*, **1205.004**
- Ram, R.S., Wallace, L., & Bernath, P.F., 2010, *Journal of Molecular Spectroscopy*, **263**, 82
- Ram, R. S., Wallace, L., Hinkle, K. & Bernath, P. F., 2010, *ApJS*, **188**, 500
- Renzini, A., & Voli, M., 1981, *A&A*, **94**, 175
- Straniero, O., Gallino, R., & Cristallo, S., 2006, *Nucl. Phys. A*, **777**, 311
- Townes, C.H., & Schawlow, A.L., 1995, *Microwave spectroscopy*, McGraw-Hill, New York, pp 9-14
- Wallerstein, G. & Knapp, G.R., 1998, *ARA&A***36**, 369
- Zamora, O., et al. 2009, *A&A*, **508**, 909
- Zhan, X., & Jeffery, C.S., 2013, *MNRAS*, in press
- Zinner, E., Ming, T. & Anders, E. 1987, *Nature*, **330**, 730

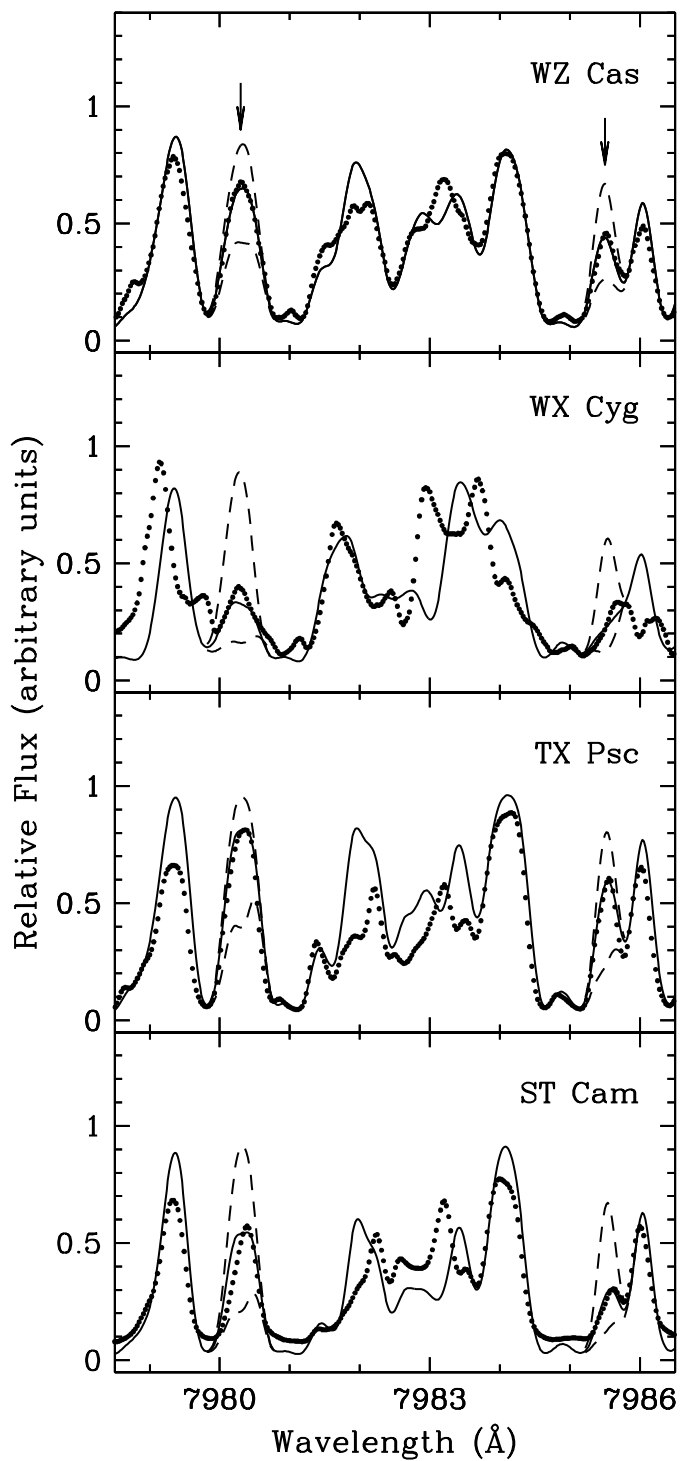


Fig. 1.— Comparison of observed (filled circles) with synthetic spectra (lines) for the stars WZ Cas (SC-type), WX Cyg (J-type), TX Psc and ST Cam (N-type). The arrows in the upper panel mark two of the $^{12}\text{C}^{15}\text{N}$ features used to derive the $^{14}\text{N}/^{15}\text{N}$ ratio. For all stars the upper dashed line represents a synthetic spectrum calculation with no ^{15}N ; the other lines

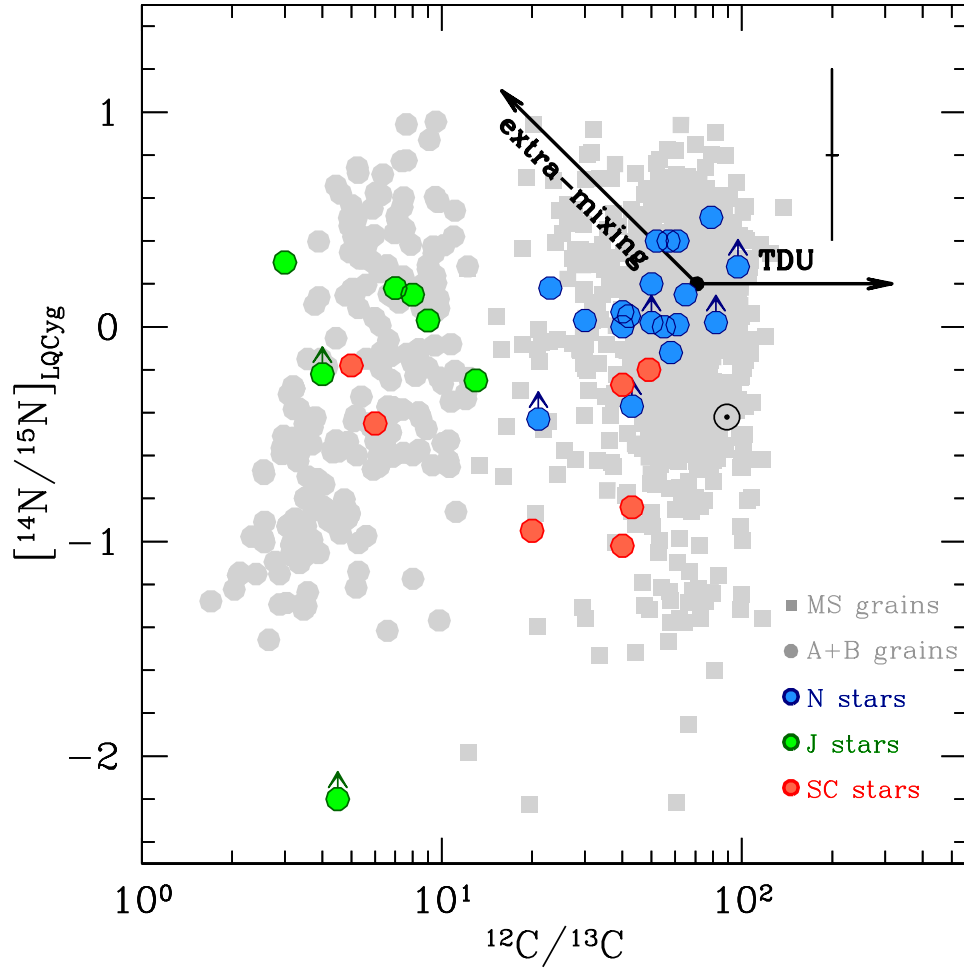


Fig. 2.— Colour circles: carbon and nitrogen isotopic ratios (relative to LQ Cyg) derived for different C star spectral types. Grey symbols: isotopic ratios measured in MS and A+B SiC grains. A typical error bar on the stellar ratios is shown. Uncertainties in the SiC grains are smaller than the data points. The black horizontal arrow indicates the theoretically expected behaviour of the C and N isotopic ratios during normal AGB evolution due to the TDU episodes. The diagonal arrow instead represents the change in the isotopic ratios when an extra-mixing mechanism during the AGB is included (see text). The black dotted circle denotes the Solar System ratios.

Table 1. Selected $^{12}\text{C}^{15}\text{N}$ lines

Wavelength (Å)	χ (eV)	$\log gf$
7980.300	0.035	-2.629
7980.357	0.035	-2.400
7985.440	0.041	-2.627
7985.501	0.041	-2.353
7985.536	0.197	-1.867
8029.694	0.184	-1.626
8029.921	0.095	-2.655
8030.014	0.095	-2.113
8037.581	0.105	-2.087
8037.733	0.197	-1.609
8063.541	0.239	-1.562

Note. — Several of these lines may contribute to the selected features in the analysis (see text).

Table 2. Nitrogen and carbon isotopic ratios

Star	S/N	$^{14}\text{N}/^{15}\text{N}]_{\text{LQCyg}}$	N_{lines}	$^{14}\text{N}/^{15}\text{N}$	$^{12}\text{C}/^{13}\text{C}$	ref
N-type						
AQ And	640	0.03 ± 0.08	3	1230 ± 260	30	2
AW Cyg	410	>-0.43	2	>750	21	4
BL Ori*	620	0.40 ± 0.20	3	3700 ± 3000	57	1
EL Aur	500	0.20 ± 0.13	4	2300 ± 1300	50	4
LQ Cyg	290	0.0	5	1170 ± 470	40	4
NQ Gem	570	0.18 ± 0.60	2	3700 ± 3900	23	5
ST Cam*	560	0.01 ± 0.29	4	1300 ± 1000	61	1
SY Per	390	>-0.37	2	>800	43	4
TX Psc*	650	0.05 ± 0.15	3	1040 ± 150	43	1
U Cam*	290	>0.28	2	>2000	97	1
UU Aur*	590	>0.02	2	>1000	52	1
V460 Cyg*	560	0.40 ± 0.29	2	4600 ± 2500	61	1
V758 Mon	370	0.05 ± 0.38	4	1600 ± 1400	65	5
V Aql*	580	>0.02	2	>1800	82	1
W Cam	630	0.07 ± 0.10	3	1300 ± 200	40	6
W Ori*	480	0.51 ± 0.45	3	4300 ± 2500	79	1
X Cnc*	220	0.40 ± 0.44	3	3300 ± 1800	52	1
Y Tau*	590	-0.12 ± 0.25	3	880 ± 190	58	1
Z Psc*	570	0.00 ± 0.45	3	1300 ± 1100	55	1

Table 2—Continued

Star	S/N	$^{14}\text{N}/^{15}\text{N}]_{\text{LQCyg}}$	N_{lines}	$^{14}\text{N}/^{15}\text{N}$	$^{12}\text{C}/^{13}\text{C}$	ref
J-type						
BM Gem	340	0.03 ± 0.55	2	1330 ± 800	9	3
RX Peg	490	0.15 ± 0.55	2	1800 ± 1100	8	3
UV Cam	440	> -0.22	2	> 700	4	3
V353 Cas	360	0.18	1	2400	7	3
V614 Mon	620	8	3
VX And*	650	-0.25	1	900	13	1
WX Cyg	230	> -2.20	2	> 6	4.5	3
Y Cvn	500	0.30	1	3200	3	3
SC-type						
GP Ori*	240	-0.27 ± 0.20	5	660 ± 360	40	6
RS Cyg	540	-1.02 ± 0.15	3	105 ± 60	40	5
RR Her	460	-0.84 ± 0.29	2	220 ± 240	43	5
RZ Peg*	260	12	6
UV Aur	260	-0.95 ± 0.14	3	125 ± 100	20	6
VX Gem	220	-0.45 ± 0.64	2	900 ± 990	6	6
WZ Cas*	380	-0.18 ± 0.25	3	640 ± 240	5	3
BD +10 3764	630	-0.20 ± 0.39	2	1100 ± 1400	49	5

Note. — S/N is the signal to noise ratio achieved at $\sim 8000 \text{ \AA}$. N_{lines} is the number of $^{12}\text{C}^{15}\text{N}$ lines used. The errors are the dispersion in N ratios when more than one $^{12}\text{C}^{15}\text{N}$ line was used. For the stars marked with an asterisk, C and O abundances were derived from the analysis of $2.2 \mu\text{m}$ spectra.

References. — Sources for $^{12}\text{C}/^{13}\text{C}$: (1) Lambert et al. 1986; (2) Ohnaka & Tsuji 1996; (3) Abia & Isern 2000; (4) Abia et al. 2002; (5) Zamora et al. 2009; (6) derived in this work.